930–941 Nucleic Acids Research, 1999, Vol. 27, No. 4

SURVEY AND SUMMARY

A general model for site-specific recombination by the integrase family recombinases

Yuri Voziyanov[1], Shailja Pathania and Makkuni Jayaram*

Department of Microbiology and The Institute for Cell and Molecular Biology, University of Texas at Austin, Austin, TX 78712, USA and [1]Institute of Molecular Biology and Genetics, Zabolotnogo 150, Kiev-143, 252143, Ukraine

Received July 9, 1998; Revised and Accepted October 9, 1998

ABSTRACT

We present here a general model for integrase family site-specific recombination using the geometric relationships of the cleavable phosphodiester bonds and the disposition of the recombinase monomers (defined by their binding planes) with respect to them. The 'oscillation model' is based largely on the conformations of the recombinase-bound DNA duplexes and their dynamics within Holliday junctions. The duplex substrate or the Holliday junction intermediate is capable of 'oscillating' between two cleavage-competent asymmetric states with respect to corresponding chemically inert 'equilibrium positions'. The model accommodates several features of the Flp system and predicts two modes of DNA cleavage during a normal recombination event. It is equally applicable to other systems that mediate recombination across 6, 7 or 8 bp long strand exchange regions (or spacers). The model is consistent with ~0–1, 1–2 and 2–3 bp of branch migration during recombination reactions involving 6, 7 and 8 bp spacers, respectively.

INTRODUCTION

Site-specific recombination of the integrase (Int) type plays a central role in the life cycles of temperate bacteriophage, bacteria and yeasts (1,2): in the integration into and excision from the host chromosome of phage genomes, in stable partitioning of plasmid, phage or bacterial genomes, in effecting developmental switches in gene expression and in the copy number control of yeast plasmids via replicative amplification (3–7). Although integrase type recombinases have not been found in higher eukaryotes, when expressed appropriately, they can act efficiently in these cell types (8–12).

The primary amino acid sequences of the Int family recombinases reveal only modest homology among them; however, secondary structural alignments indicate large conservation of peptide motifs within which specific residues have been retained throughout the family (13,14). Recently solved crystal structures of λ Int, HP1 Int (integrase from the λ-related *Haemophilus* phage), XerD and Cre proteins are suggestive of approximately equivalent three-dimensional organization of all the Int family members (15–18). A hallmark of the family is an invariant active site tetrad, consisting of two arginines, one histidine and one tyrosine (19,20). The tyrosine residue (Tyr343 in the Flp recombinase) is responsible for breaking the DNA chain to form a 3′-phosphotyrosine bridge and expose an adjacent 5′-hydroxyl group. The phosphotyrosine bond then becomes the target of attack by the 5′-hydroxyl group from the cleaved strand of the partner DNA during the strand joining step of recombination. The RHR triad (Arg191, His305 and Arg308 in Flp) is presumably responsible for the orientation of the scissile phosphodiester bonds at both these steps.

The core recombination sequences, within which phosphoryl transfer reactions occur, show a similar organizational pattern for the family. They consist of two inverted recombinase binding elements separated by a 6–8 bp spacer region. Strand cleavage and exchange at the left and right borders of the spacer are temporally separated. Consequently, recombination is completed in two steps of single-strand exchanges, a Holliday junction being an obligatory intermediate in the reaction. Within this unified mechanistic scheme, individual recombinases of the family may differ in specific details of the reaction. For example, it appears that the mode of strand cleavage (whether the tyrosine nucleophile from a DNA-bound recombinase monomer is utilized *in cis* to cleave the labile phosphodiester bond adjacent to it or *in trans* to cleave the one distal to it across the spacer) is not uniform (18,21–28).

A theoretical analysis of a set of Int family recombination targets shows a similar pattern of DNA bendability in their spacer regions and in their protein binding elements (29). In the Flp system, alterations of the polypyrimidine tracts harboring the scissile phosphates result in reduced recombination efficiency (30). Furthermore, the large DNA bend induced within the spacer by an Flp dimer bound to the recombination target site is primarily responsible for the selective assembly of only one of the two possible active sites and provides a geometric basis for the two-step strand exchange mechanism (31–34). Upon association with an Flp variant that cannot cleave DNA, pre-formed Holliday structures adopt an 'unstacked and extended conformation' that is conducive to potential branch migration within the spacer (35,36). This roughly square-planar arrangement of the recombinase–Holliday junction complex is also supported by the crystal structure of Cre bound to its target DNA (18,37). Overall, the available information implies that the DNA substrate is not just a passive target for strand breakage and joining by the recombinase; rather, it actively contributes to the mechanistic course of the reaction.

*To whom correspondence should be addressed. Tel: +1 512 471 0966; Fax: +1 512 471 5546; Email: jayaram@almach.cc.utexas.edu

The general model for Int family recombination proposes that the double helical geometry of DNA, its bendability and its oscillatory movement within the overall structure of the recombination complex fosters recombinase configurations that permit coordinated cleavage/exchange reactions selectively at the left or right ends of the spacers. The final picture accommodates features of the Stark *et al*. proposal for enzyme–DNA movements during recombination that account for the difference in strand exchange topologies between integrase and resolvase/invertase systems (38). It is also consistent with several experimental observations related to the mechanics of recombination by Int, XerC/XerD and Cre (18,24,39).

RESULTS AND DISCUSSION

DNA–protein contributions in Int family recombination: general considerations

The 'minimal' DNA substrate of the Int type recombinases (depicted in Fig. 1A) includes two oppositely oriented binding elements spaced 6–8 bp apart, each of which binds a monomer of the recombinase. The relative positioning of the labile phosphates when viewed down the barrel of the DNA cylinder is shown in Figure 1B. For a 6 bp spacer (as in the Cre substrate), the two phosphates would be virtually superimposable and for an 8 bp spacer (as in the Flp substrate) they would be offset by ~72°. Additional features such as bipartite DNA binding targets for the recombinase protein, extra recombinase binding elements on one side of the minimal substrate or separate binding sites for accessory protein factors (found in a subset of the recombination systems) will not be considered here in developing a general model for Int family recombination. In the case of Flp, binding of two protein monomers to a DNA target results in a large bend, centered within the spacer and estimated to be >140° as measured by gel mobility comparison with bent DNA standards (31,32,40). The DNA bend is consistent with the assembly of the Flp active site at the interface of the two monomers bound on either side of the spacer. Point mutants of Flp that bind DNA normally but cannot induce the sharp bend (likely reflecting a weakening of the monomer–monomer interactions) are defective in the chemical steps of recombination (31,40,41). When the geometric constraints normally posed by the spacer DNA are mitigated, either by using half-site substrates or by providing a prebent full-site substrate, a bending-incompetent mutant becomes cleavage proficient (34,40,42).

The first strand cleavage/exchange reaction between two DNA target sites will produce a Holliday intermediate, in which four helical arms flank the crossover point (Fig. 1C). It is reasonable to imagine that the conformation of this four-way junction within the recombination complex would be critical to the second strand exchange reaction that yields the mature recombinants. Experiments with the Int and the XerC/XerD systems, using Holliday substrates constrained to adopt one of two possible 'cross-strand' isoforms by a sequence-dictated design or by physically tethering strands, suggest that switching of the junction between two stacked X-forms constitutes a requisite isomerization step in the recombination reaction (43,44). In contrast, the crystal structure of a complex formed by the Cre protein with a 'nicked' or nick-free Holliday junction reveals a roughly square-planar arrangement of the helical arms (37). Studies using a cleavage-incompetent variant of Flp is also consistent with an extended, nearly planar form of the Holliday junction in its protein-bound form (35). The representation in Figure 1C approximates this conformation. In this structure, the cleavage points are related to each other by a four-fold axis of symmetry. When the Holliday junction is viewed from the side (Fig. 1D), the scissile phosphates are seen to be positioned roughly in one plane and towards one side of the structure (in this view, they face the bottom of the page).

The oscillation model is concerned with the conformational dynamics within the 'symmetric' or 'equilibrium' state of the Holliday structure represented by the extended conformation (Fig. 1C; 36) that bring alternative pairs of the scissile phosphates into their cleavage-competent configuration. The term 'equilibrium state or position' does not imply that the four-fold symmetric Holliday junction is a stable intermediate in the recombination pathway. Rather, it likely represents a transient state traversed by the recombination complex during its switch between the chemically active states that catalyze strand cleavage and exchange at either end of the spacer.

'Binding site' planes and their relative orientations

First, within a cylindrical representation of the DNA substrate, we define two types of binding site planes, plane 1 and plane 2 (Fig. 2). For the purposes of the model, these planes may be considered as synonymous with two rectangular surfaces (outlined in red and green in Fig. 2) restricted by the edges of the cylinder and the boundaries of the recombinase binding elements. Our intent is to generalize, across the family, the interaction between a recombinase monomer and its cognate DNA element (plane 1 or Va), as well as that between two recombinase monomers bound to the left and right DNA arms, respectively (plane 2 or Vc). A common recombinase–DNA interaction is justified, based on the conserved overall three-dimensional peptide folds for the individual proteins revealed by the crystal structures (15–18) and the nearly constant size (11–13 bp) of the binding site. Similarly, a uniform mode of dimer interaction in catalysis is assumed, based on a number of results with the Flp system that are in general agreement with the protein contacts seen in the Cre–DNA structure (18,21,28,34,37). However, since the protein monomers at the left and right arms are separated by 6–8 bp of the double helix in individual systems, the dynamics of the spacer in establishing the catalytically relevant dimer interaction would be critical in accounting for a common recombination mechanism.

Plane 1 is the spanning surface bounded by the two mutually perpendicular vectors, Va and Vb, originating at the cleavage point (indicated by the red knob) and their respective parallel translations at the distal end of the binding element and the distal surface of the cylinder (Fig. 2A and C, rectangles with the red border). Assuming that there are no sequence-dependent changes in the periodicity of the double helix, the relative orientations of Va (Va^L and Va^R) within a recombination substrate are determined solely by the length of the spacer region. When viewed from one end of the cylinder, the angular displacement between Va^L and Va^R will be close to 0° for Cre (6 bp spacer), 36° for Int (7 bp) and 72° for Flp (8 bp) (Fig. 2B).

Plane 2 is defined in the following way. First, we superimpose the recombination targets from the Int family such that the centers of their spacer regions become coincident and construct a vector Vc that bisects Va^L and Va^R (Fig. 2B). When these DNA molecules are viewed from one end of the cylinder along the helix axis, the cleavage points from each molecule will be symmetrically

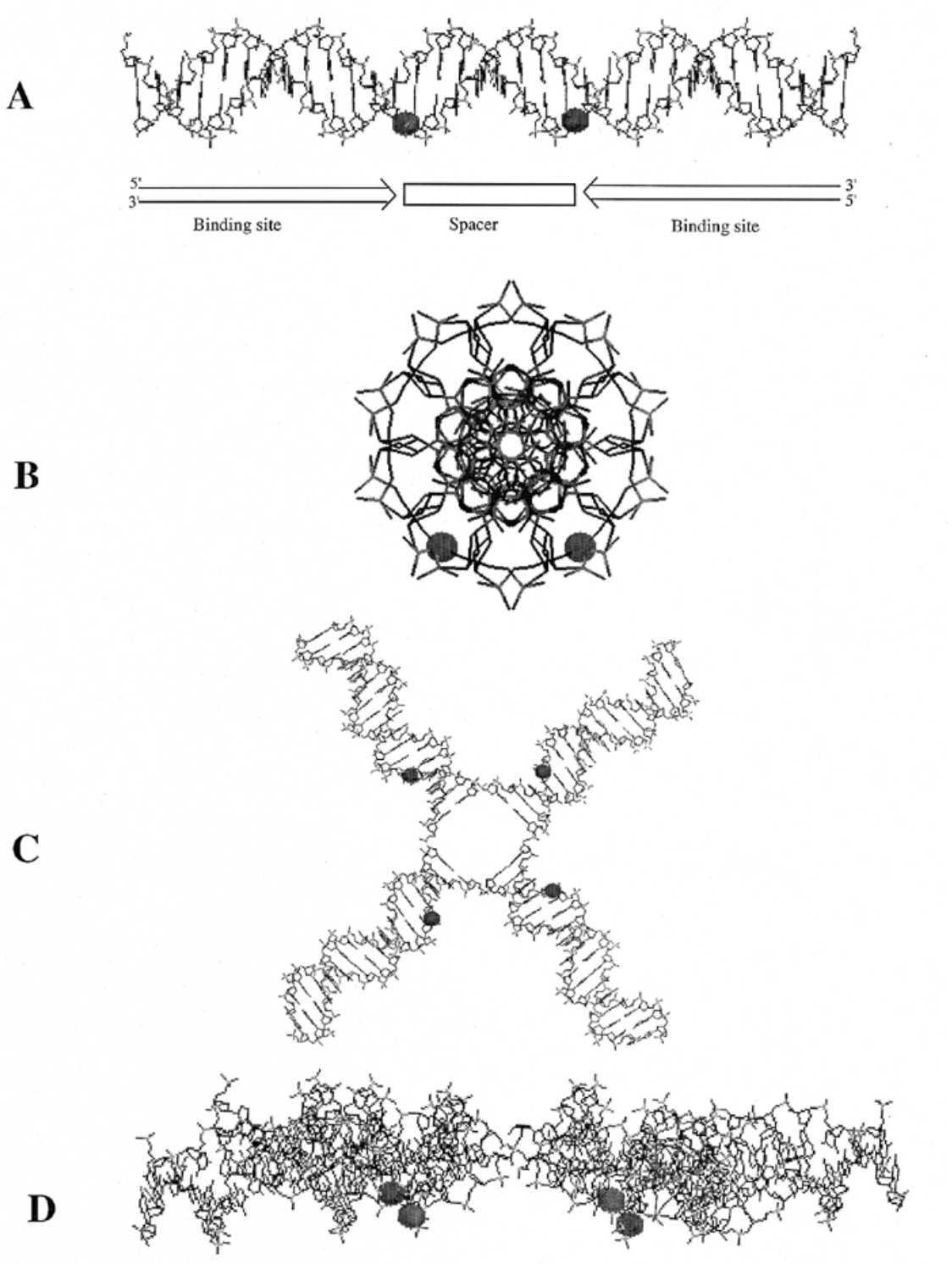

Figure 1. Structural features of the Int family recombination substrate and the Holliday junction intermediate. (**A**) The minimal recombination target site consists of two recombinase binding elements flanking the strand exchange region (spacer). The binding elements are arranged in a head-to-head orientation. In the case of the Flp substrate, the phosphates at the cleavage sites (dark circles) on the two strands are separated by 8 bp. (**B**) When the substrate is viewed from one end along the DNA axis, these phosphates subtend an angle of ~72° at the helix axis. (**C**) The first strand exchange between two molecules of the substrate shown in (A) produces a Holliday junction intermediate. In its four-fold symmetric form, the scissile phosphates will be equidistant from the center of the branch point. (**D**) When the Holliday junction in (C) is viewed from its side, these phosphates lie essentially in one plane. In reality, two of the phosphates at the back will be eclipsed by the two in the front. The structure is slightly tilted to make all four visible.

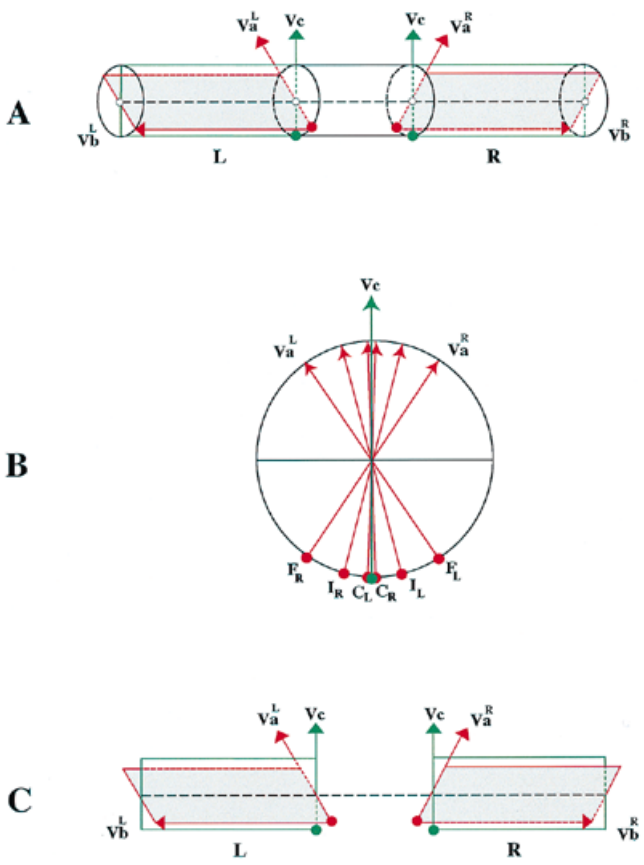

Figure 2. The binding planes within a recombination target. (**A**) The binding planes 1 and 2 (described in the text) are shown by their red and green borders, respectively. L and R refer to the left and right binding sites, respectively. The angular displacement between the left and right binding planes 1 (between Va^L and Va^R) is dependent upon the spacing between the labile phosphates (or the spacer length), while that between the left and right planes 2 (between Vc^L and Vc^R) is 0. The helix axis is indicated by the dashed line. (**B**) The dispositions of Va^L and Va^R for three of the Int family recombinases Flp (F), Int (I) and Cre (C) relative to Vc are clearly seen in this view from the left end along the DNA axis. The cleavage points at the left and right ends are denoted by the subscripts L and R, respectively. (**C**) The orientation of planes 1 and 2, when removed from the cylindrical DNA frame, is shown.

arranged to the left and to the right of Vc (Fig. 2B). Plane 2 can be obtained by parallel translations of this vector to the start and end points of a recombinase binding element as shown in Figure 2A and C (rectangles with green border).

In order to simplify the overall description of the model, we shall replace plane 1 and plane 2 by the two vectors Va and Vc that represent them (see below). However, in defining the functional relationship between two recombinase monomers bound to neighboring DNA arms, it is important to note that there are two sides to each plane, a 'left' and a 'right' side; indicated by gray and dark shades, respectively, in Figure 3.

We shall assign arbitrary directions to the planes 1 and 2: the arrowheads on Va and Vc represent the 'top', the green and red knobs represent the bottom. The angular displacement between plane 1 and plane 2 (the angle between Va and Vc) at a binding element is a function of the spacer length (just as is that between Va^L and Va^R). The magnitude of this displacement is ~0° for Cre, 18° for Int and 36° for Flp.

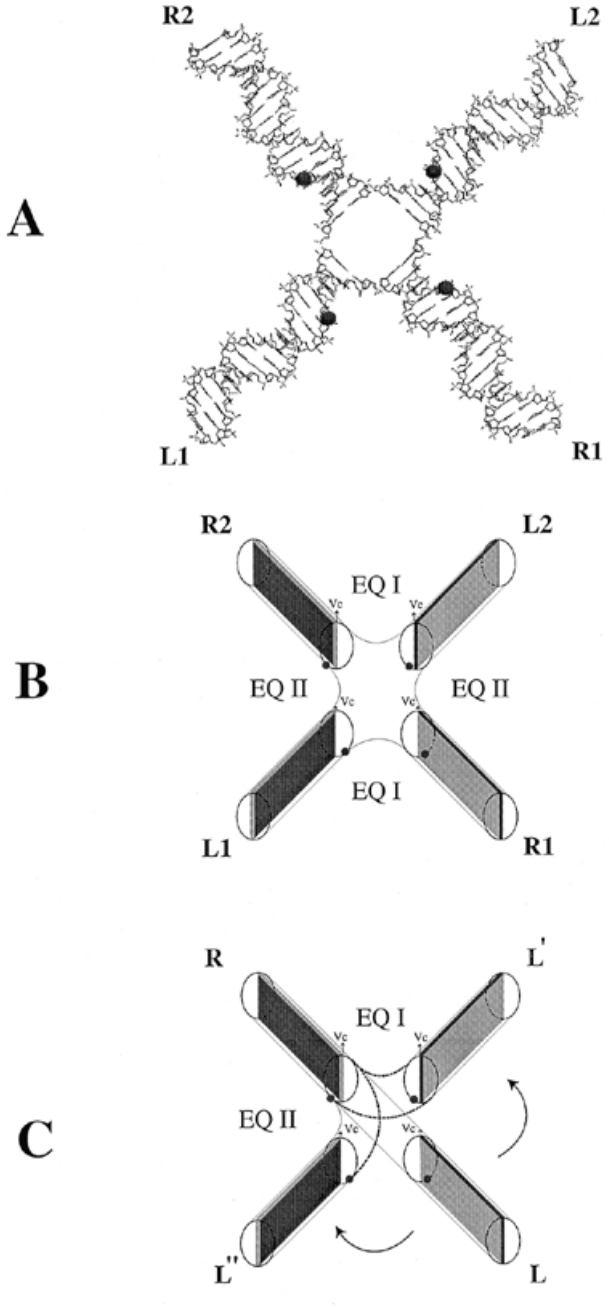

Figure 3. The nearly four-fold symmetric square-planar Holliday intermediate in Int family recombination. (**A**) A potential intermediate during Int type recombination reactions is the nearly square-planar Holliday junction in which all cleavage points are located at the same distance from the branch point. In principle, this structure may be arrived at following the first cleavage/exchange reaction at the left or at the right end of the spacer between two linear substrates. L and R refer to the left and right recombinase binding arms, respectively. (**B**) The junction in (A) is shown by its cylindrical representation. The binding planes 2 at the four arms are each indicated by the direction of the vector Vc for each of them. In this equilibrium state, none of the four labile phosphodiester bonds are in the cleavable condition. Note that the structure is only pseudo-symmetric. The L1-R1 and L2-R2 arms are in the EQ I state, in which the right side (shown in dark) of the left plane faces the left side (shown in gray) of the right plane. On the other hand, the L2-R1 and L1-R2 arms are in the EQ II state, in which the left side of the left plane faces the right side of the right plane. (**C**) From a linear substrate LR, the EQ I and EQ II states can be established by bending the L arm counterclockwise to the L′ position or clockwise to the L″ position. L, L′ and L″ correspond, respectively, to R1, L2 and L1 in (B).

We may now analyze the geometric transitions of DNA arms (and the bound recombinases) during recombination in terms of either Va (plane 1) or Vc (plane 2) without affecting the relevant conclusions. However, the constant orientation of Vc, by definition, makes it the preferred choice when considering those features of the reaction that apply globally to all of the Int family systems. Features that distinguish one system from another are best illustrated in terms of Va.

Transitions of the recombination complex between cleavage-incompetent and cleavage-competent states

Imagine a Holliday structure formed by the exchange of one pair of strands between two DNA substrates L1R1 and L2R2. In its planar four-fold symmetric configuration (Fig. 3A and B), the vector Vc for a given binding site is parallel to the Vc for the other three binding sites as well. Recent insights provided by the Cre–DNA crystal structure (18,37) and by Flp(Y343F)-bound Holliday junctions (35) suggest that this conformation is a plausible intermediate, albeit a transient one, in the Int family recombination pathway. It is important to realize that the structure is (in a strict sense) only pseudo-symmetric, since (as already pointed out) a binding site plane has two sides to it: left shown in gray and right shown in dark. In the parental pair of arms (L1-R1 and L2-R2), it is the dark side from the left arms that faces the gray side from the right arms. In the recombinant pair of arms (L1-R2 and L2-R1), it is the gray side from the left arms that faces the dark side of the right arms. [The gray and dark sides are defined from the standpoint of an observer at the distal end of a DNA arm (with Vc directed upward) and looking towards the branch point along the axis.] The difference is easily seen in Figure 3C, where a linear DNA target site is bent in one of two possible ways. We can now designate an equilibrium state EQ, with two substates EQ I and EQ II, that adequately describe the parental and recombinant arm dispositions within the cleavage-incompetent Holliday intermediate with pseudo four-fold symmetry. L1-R1 and L2-R2 arms conform to EQ I, whereas R1-L2 and R2-L1 arms conform to EQ II. The two states are related by the same orientation of Vc, but they are distinguished by how the binding planes defined by Vc face each other.

It might seem simpler to define a single equilibrium state EQ for the apparently four-fold symmetric junction rather than the two substates EQ I and EQ II described above. However, it is important to note the functional non-equivalence between EQ I and EQ II. As will become clear in the analysis below, EQ I and EQ II are the precursor states for two distinct cleavage conditions. One targets the scissile phosphate at the left end of the spacer, the other targets the scissile phosphate at the right end. The two-fold symmetry observed in the structures of an immobile Holliday junction bound by a catalytic mutant of Cre and a nicked Holliday junction bound by wild-type Cre is consistent with the EQ I/EQ II dual states (37).

Escape from the pseudo-four-fold symmetry and establishment of cleavage conditions are possible, in principle, by rotation of the DNA arms (equivalent to branch migration) and the consequent changes in the relative orientations of Vc, by scissor-like motion of the arms that alter the bend angle between adjacent arms or by reconfiguration of the square-planar Holliday junction into a stacked X-form or by combinations of these conformational alterations. Based on results with Cre and Flp (18,35,37), we have focused our attention on the planar form of the Holliday junction and not on the stacked X-form. Since current models for Flp and Int recombinations invoke at least limited branch migration (35,39,45,46), we shall consider how DNA rotations can modulate interactions among the bound recombinase monomers.

The oscillation model for Int family recombination

The four arms (L1, R1, L2 and R2) of the symmetric junction (EQ I/EQ II; see Fig. 3A and B) are represented by the corresponding Vc vectors in Figure 4A. DNA rotation (depicted in Fig. 4B and C) will result in branch migration, causing one pair of cleavage points to move towards and the other pair to move away from each other. The sense of rotation of the arms (clockwise or counterclockwise) will determine which pair of cleavage points approach each other and which ones recede from each other. Thus, along with their rotational reorientation, the Vc vectors (and the corresponding recombinase monomers) will experience simultaneous linear displacement as well. Thus, it is the two-fold realignment between pairs of recombinase monomers that is the basis for the oscillation of the reaction complex between two cleavage states via the equilibrium state.

The consequence of rotating the left arms in the clockwise and the right arms in the counterclockwise direction from the equilibrium state (Fig. 4A) is depicted in Figure 4B. The transitions of EQ I and EQ II are indicated by the thick arrows (Fig. 4A and B). The top ends (arrowheads) of Vc^L1 and Vc^R1 approach each other, as do those of Vc^L2 and Vc^R2. Thus, the L1-R1 and L2-R2 arms shift from the EQ I state (Fig. 4A) and enter the P1 zone, defined by the inclination of two neighboring Vc vectors in which the arrowheads are proximal and the knobs are distal to each other (Fig. 4B). Continued rotation will, at 90°, bring each of the two Vc^L/Vc^R pairs in direct opposition. We call this state, with the two adjacent arrowheads in closest proximity, the switch point, SP-P. The sectors delimited by EQ and SP-P in Figure 4B, highlighted by the thick arcs, represent the P1 zone. Let us arbitrarily assume that, for a given recombination system, the cleavage state is arrived at by the arrowheads of two adjacent Vc vectors tilting towards each other (representing a catalytically active dimer interface). Let us further assume that the pair of scissile phosphates at the left end (top strands) or at the right end (bottom strands) of the spacer assume cleavage competence by migrating towards each other (as opposed to migrating away from each other). In the case depicted in Figure 4B then, the P1 zone resulting from the rightward swing of Vc^L1 and Vc^L2 and the leftward swing of Vc^R1 and Vc^R2 will harbor the specific reactive state for the left cleavage points.

The transition from equilibrium by counterclockwise rotation of the left arms and clockwise rotation of the right arms is depicted by the hatched arrows (Fig. 4A–C). The resultant P2 zones (established by the leftward swing of Vc^L1 and Vc^L2 and rightward swing of Vc^R1 and Vc^R2) will contain the cleavage state for the right cleavage points. The P2 zones are depicted in Figure 4C by sectors highlighted by the thick arcs.

The schematics in Figure 4 also illustrate the ‘complementary’ relationship between the P and F zones: when P is the cleavage zone, F is the non-cleavage zone. In the F zones, it is the bottom knobs of Vc vectors that approach each other; they attain their closest disposition at the switch point SP-F. As shown in Figure 4B, when the L1-R1 and L2-R2 pairs of arms are in the P1 zone, the R1-L2 and R2-L1 pairs are in the F2 zone. In other words, when the scissile phosphates at the left spacer end are in the cleavable zone (P1; P is for cleavage-permissive, the suffix 1 is for the left end), those at the right end are in the non-cleavable zone

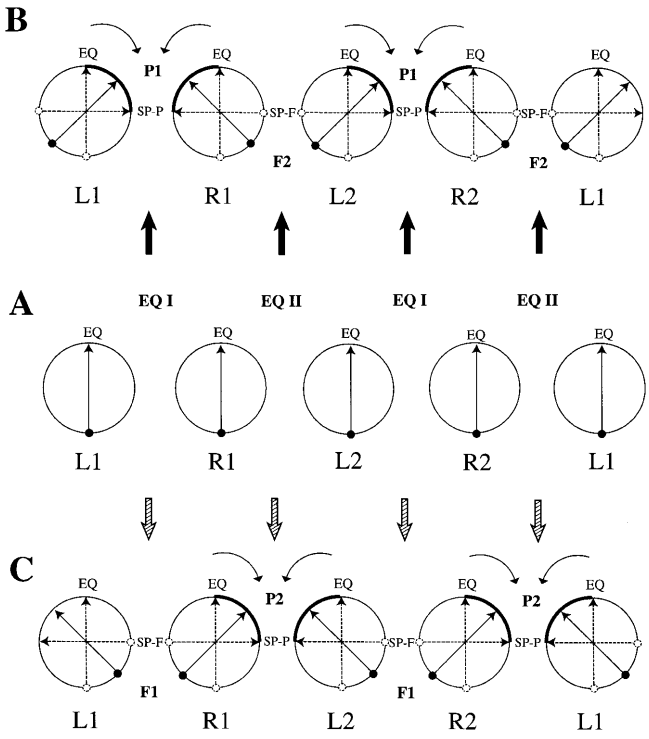

Figure 4. Orientation of the binding planes and their displacement by DNA rotation in the Holliday junction intermediate. The effects of DNA rotation on the binding planes of adjacent pairs of DNA arms of the Holliday junction are schematically diagrammed. The arrows within the circular arm cross-sections represent the vectors Vc (binding planes 2). (**A**) In the four-fold symmetric state of the Holliday junction (see Fig. 3B), Vc is oriented in the same direction (arrowhead pointed upwards) in all four arms, regardless of whether a pair of adjacent arms are in the EQ I state or in the EQ II state. Under this non-cleavable condition, the L1-R1 and L2-R2 arms assume the EQ I configuration (the right side of Vc^L facing the left side of Vc^R) and the R1-L2 and R2-L1 arms assume the EQ II configuration (the right side of Vc^R facing the left side of Vc^L). (**B**) For a recombinase that cleaves in the P zone, clockwise rotation of the left arms and counterclockwise rotation of the right arms (branch migration of the left cleavage points towards each other) establish the P1 cleavage zone (sectors denoted by the bold arcs) for the L1-R1 and L2-R2 arms. The interactions between the recombinase monomers at each of these pairs of arms are of the *trans*-horizontal type (21). At the same time, the R1-L2 and R2-L1 arms are placed in the cleavage-free F2 zones. Recombinase interactions at these arm pairs are of the *trans*-diagonal type (21). Hence the P1/F2 zone combination represents productive *trans*-horizontal interactions and non-productive *trans*-diagonal interactions. The positions of Vc at the limits of the P1 and F2 zones (the switch points SP-P and SP-F, respectively) are indicated by the dashed lines. (**C**) Clockwise rotation of the right arms and counterclockwise rotation of the left arms (branch migration of the right cleavage points towards each other) will place the R1-L2 and R2-L1 arms in the P2 cleavage zones (sectors with the bold arcs) and the L1-R1 and L2-R2 arms in the cleavage-free F1 zones. Therefore, in the P2/F1 zone configuration, *trans*-diagonal interactions are fruitful and *trans*-horizontal interactions are futile. The switch points SP-P and SP-F are indicated as in (B).

(F2; F is for cleavage-forbidden, the suffix 2 is for the right end). Furthermore, the productive recombinase interaction for left end cleavages is established by the L1-R1 dimer and the L2-R2 dimer. At the same time, the R1-L2 and R2-L1 dimers are in the non-cleaving configuration. Similarly, as represented in Figure 4C, when the R1-L2 and R2-L1 pairs of arms are in the P2 zone, the L1-R1 and L2-R2 pairs are in the F1 zone. Correspondingly, when the right end phosphodiesters are cleavable (P2) by the R1-L2 and R2-L1 dimers, the left end phosphodiesters are non-cleavable (F1) by the L1-R1 and L2-R2 dimers (Fig. 4C).

Note that, in the movement of DNA arms, the relevant entities are the recombinase-bound DNA arms. Branch migration within a Holliday junction formed between DNA partners with homologous spacers is an isoenergetic process, loss of base pairing in one segment being compensated by gain of base pairing in another. The associated sliding and rotation of the recombinase monomers, however, will result in remodeling of intersubunit interactions and, in principle, may modify protein–DNA contacts as well. Assuming that the two-fold symmetric states of the complex that execute the chemical steps at the two spacer ends are equivalent, interconversion between these states must also be isoenergetic, since interfaces that are disrupted would be replaced by equivalent new ones. The overall energy cost of the process must be close to zero, since Int family recombination occurs without exogenous supply of energy. This would be a reasonable scenario, provided the movements are relatively short range (involving a few base pairs of DNA and relatively small scale protein interactions).

For the special case discussed in Figure 4, we assumed that the P zone is the cleavage-permissive zone (the F zone therefore being the cleavage-forbidden zone) and that branch migration selectively promotes the cleavage of one pair of scissile phosphodiester bonds by increasing their proximity. In the general case, though, there are three other possibilities. For example, in the P zone cleavage state, it could be the distant pair of scissile phosphates that become cleavage susceptible. Alternatively, the F zone (and not the P zone) might represent the cleavage zone, with either the proximal or the distal pair of phosphodiesters being the cleavage-susceptible ones. Note that, by setting the switch points SP-P and SP-F as the endpoints of oscillation in Figure 4, we have limited the relative rotation between two adjacent DNA arms to ≤180° (90° + 90°). Setting this limit is not an absolute requirement of the model. However, it would seem that the structural constraints within the recombinase-bound Holliday junction are likely to impede (if not forbid) violation of the switch point barrier.

We wish to re-emphasize that the cleavage zone (whether it is P or F, depending on the recombination system) refers to a pair of neighboring left and right DNA arms bound by the recombinase (Fig. 4B and C). The underlying implication here is that the catalytically active form of the protein is a dimer and that this dimer is constituted by one monomer bound to an L arm and the second monomer bound to an adjacent R arm. This feature of the oscillation model unifies all Int family members in their catalytic associations, regardless of whether they utilize the active site tyrosine *in cis* or *in trans*. For Flp, it has been demonstrated that a dimer is cleavage competent and that this reaction is not dependent on synapsis between two DNA substrates (47).

Relating DNA rotation in a Holliday junction to that in a linear substrate

It is now pertinent to ask whether the rotational movements proposed for the Holliday junction are relevant to a linear substrate as well. We shall first rotate a two armed DNA substrate bent in the EQ I state (position of the bend is central to the spacer; Fig. 5A) in a right-handed fashion as seen from the distal end of the L arm (clockwise rotation of L and counterclockwise rotation of R; Fig. 5B). Notice that, depending on the direction of rotation, the bend position may be displaced either to the right or to the left

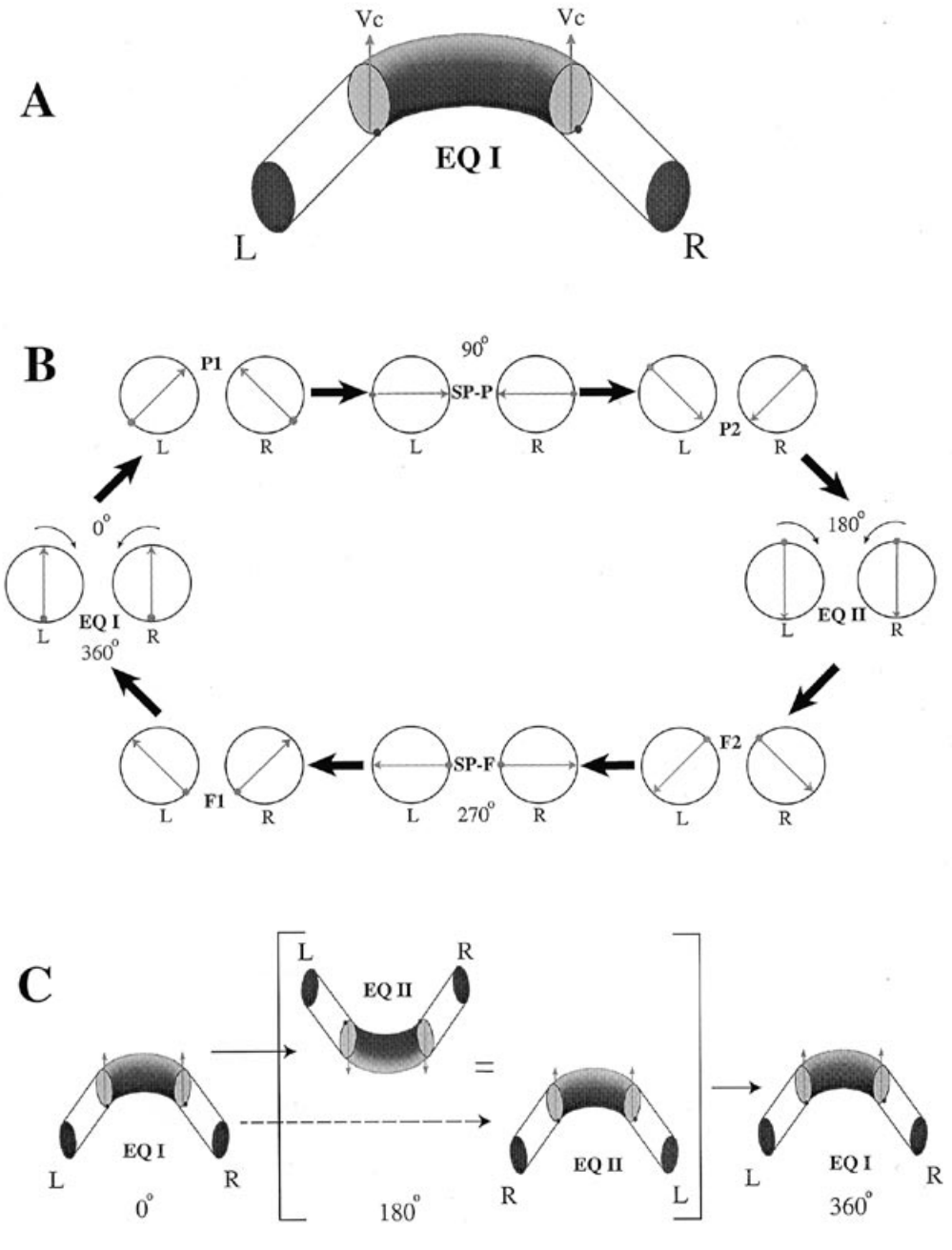

Figure 5. Relative angular displacement of binding planes upon rotation of a linear recombination target. (**A**) The linear substrate LR is bent into the EQ I state as in the Holliday junction shown in Figure 3B, with the cleavage points (dark circles) facing the bottom of the page. The direction of Vc denotes that the binding planes are oriented upwards. (**B**) Upon simultaneous clockwise and counterclockwise rotation, respectively, of the L and R arms, the DNA enters the P1 zone, crosses the switch point SP-P into the P2 zone and reaches EQ II at 180°. When rotation is continued from the EQ II state, the DNA enters the F2 zone, crosses the second switch point SP-F into the F1 zone and returns to EQ I at 360°. (**C**) The relative geometry of the DNA arms at the start point (EQ I) and following 180° (EQ II) and 360° (EQ I) rotations are schematically shown. Note the distinct relative orientations of the DNA bends in EQ I and EQ II. The representation of EQ II at the right is obtained by turning that at the left through 180° about an axis perpendicular to the plane of the paper.

of the center (see also Fig. 8 and the related segment of text). This would be analogous to branch migration in the Holliday structure with the accompanying rotation and sliding of recombinase monomers. However, to follow the rotational consequences diagrammed in Figure 5B and C, it is not strictly necessary to consider the change in the bend location. Through the first 90°, the arrowheads on Vc approach each other (while the knobs on Vc move away from each other), establishing the P1 zone as shown earlier in Figure 4B for the Holliday junction. At 90°, the switch point SP-P, the rotational limit set for the Holliday junction, is reached. During further rotation, the arrowheads still retain their relative proximity (P2 zone) until, at 180°, EQ II is established. During the next 90° rotation (F2 zone; Fig. 5B), the knobs on Vc get closer to each other, the arrowheads move apart

and, at 270°, the switch point SP-F is reached. In the SP-F state, the bottom edges (the knobs on Vc) attain their closest disposition (see also Fig. 4B and C). Completion of one full round of rotation returns the system to EQ I via the F1 zone. The relative positioning of the L and R arms in the EQ I and EQ II states during the 360° rotation cycle are shown in Figure 5C.

Several interesting points emerge by comparing Figures 4 and 5. First, entry into P1 from EQ I requires clockwise rotation of the L arm and counterclockwise rotation of the R arm (Figs 4B and 5B). Direct transition from P1 to P2 is possible only by crossing the switch point (Fig. 5B); however, P2 can be accessed from EQ II by counterclockwise rotation of the L arm and clockwise rotation of the R arm (Figs 4C and 5B). Furthermore, as shown in Figure 5C, EQ I and EQ II (derived from EQ I by 180° rotation via the switch point) can be distinguished by the oppositely directed bends of the L and R arms. This is easily seen by comparing EQ I with the left representation of EQ II in Figure 5C. One type of DNA bend may give rise to cleavage at one end of the spacer (say, by EQ I→T1 transition), whereas the other type may yield cleavage at the other end of the spacer (by EQ II→T2 transition). In the case of Flp, selective cleavage at the left or at the right end of the spacer has been demonstrated by oriented DNA bends induced by strand-specific base bulges (34). Thus, for a recombination system that has no preference for one type of bend over the other, the reaction can be initiated by cleavage and exchange at the left or at the right end of the spacer. As a corollary, an intrinsic bias towards one bend orientation can impose a defined order of strand exchange on the reaction. Figure 5C also indicates that EQ I→EQ II transition is feasible even in the absence of DNA rotation. Starting with EQ I (0°; Fig. 5C), the L and R arms can be simply reoriented to obtain the EQ II representation on the right in Figure 5C (indicated by the dashed arrow). During a recombination reaction initiated by two DNA substrates bent, say, in the EQ I/P1 format, it may be sterically impossible for the same substrate arms to bend oppositely into the EQ II/P2 format within the cross-stranded Holliday intermediate. However, the left arm of one substrate and the right arm of the other would be almost perfectly placed to implement the EQ II/P2 bend that can then facilitate the second cleavage required for completion of recombination.

Validity of the model: application to specific systems

The operation of the oscillation model on an 8 bp spacer (say, the Flp system) is illustrated in Figure 6. The choice of Flp as the example stems from the fact that the productive dimer interaction is manifested as DNA cleavage by Tyr343 in a left to right or right to left direction (Flp bound to the right arm cleaving the phosphate at the left end of the spacer or vice versa).

Within the synaptic structure, the two substrates L1R1 and L2R2 (Fig. 6A) assume the cleavage-competent P1 state (Fig. 6B) (corresponding to clockwise rotation of the L arms from EQ I). Strand breakage and exchange can occur at the left ends of the spacer by the *trans*-horizontal mode (the Flp monomers bound at the R1 and R2 arms donating Tyr343 to those bound at the L1 and L2 arms, respectively). The Holliday junction enters the P2 zone (Fig. 6D) via the non-reactive EQ I/EQ II state (Fig. 6C). In the P2 cleavage state, the Flp dimers at the R1-L2 and R2-L1 arms are in their reactive configuration; those at the L1-R1 and L2-R2 arms are in the non-reactive F2 zone configuration. The resolution step utilizes Tyr343 from L2 to cleave at R1 and from L1 to cleave at R2. The cleavage mode, by definition, is *trans*-diagonal (contribution of Flp monomers from the left arm of one parental DNA and the right arm of the other; 21).

A striking outcome of the analysis of Flp recombination by the oscillation model is that it predicts bimodal cleavage by Flp during recombination: *trans*-horizontal to initiate recombination and *trans*-diagonal to resolve the Holliday intermediate. This feature of the model is consistent with the observation of *trans*-horizontal cleavage by Flp in linear substrates (28) and *trans*-horizontal or *trans*-diagonal cleavage in Holliday junctions (48,49). The oscillation model agrees with the finding that each of the two cleavage/exchange steps of recombination requires the cooperative action of all four Flp monomers (50).

Bimodal DNA cleavage and the 'trimer model' for Flp recombination

A trimer of Flp bound to three DNA arms is capable of assembling two active sites simultaneously (48,51). Based on this finding, the Qian–Cox trimer model for Flp recombination (51) proposes that the initiation step and the resolution step are mediated by two sets of Flp trimers (Fig. 7). The composite of the Flp trimers required for the full reaction can be arranged into a cyclical tetramer pattern that superficially resembles the protein pattern observed in the Cre crystal structure (18). We wish to point out that this apparent similarity is misleading.

According to the trimer model, with the DNA arms arranged in the parallel fashion (as was represented by Qian and Cox; 51), two cleavage modes are required for strand breakage at one end of the spacer. In Figure 7A, these are: one *trans*-horizontal cleavage and one *trans*-vertical cleavage. (The same result can be achieved by one *trans*-diagonal cleavage and one *trans*-vertical cleavage). In contrast, in the oscillation model, it is only one cleavage mode (say, *trans*-horizontal) that is utilized to break the phosphodiesters at one end of the spacer (Fig. 7B). Bimodality, in this case, arises from a different cleavage mode (say, *trans*-diagonal) utilized to break the phosphodiesters at the other end of the spacer. Thus, in the trimer model, cleavage at each step of the recombination reaction is bimodal. In the oscillation model, cleavage at each step of recombination is unimodal; only for a full round of recombination does cleavage become bimodal. The trimer model is absolutely dependent upon *trans*-vertical cleavage (requiring an active L1-L2 or R1-R2 dimer; Fig. 7A or C), a cleavage mode that has not been detected with Flp (28,48), is not suggested by the Cre structure (18,37) and is virtually excluded by the oscillation model. The utilization of all four Flp monomers for each pair of strand cleavages in the oscillation model (as opposed to three monomers in the trimer model) is consistent with the finding that the catalytically relevant entity for the resolution of a Holliday junction bound by four Flp monomers is an Flp tetramer, not an Flp trimer (50). When the substrates are aligned in the antiparallel fashion (as is the case in the crystal structure of the Cre–DNA complex), the geometric relatedness between the Cre tetramer and the Flp tetramer of the oscillation model is obvious (Fig. 7B). At the same time, the discrepancy with the Flp trimer becomes quite apparent (Fig. 7C).

Role of spacer homology and extent of branch migration in Int family recombination

The structure of the cleaved Cre–DNA complex indicates that, in this roughly square-planar Holliday-like intermediate, the catalytic

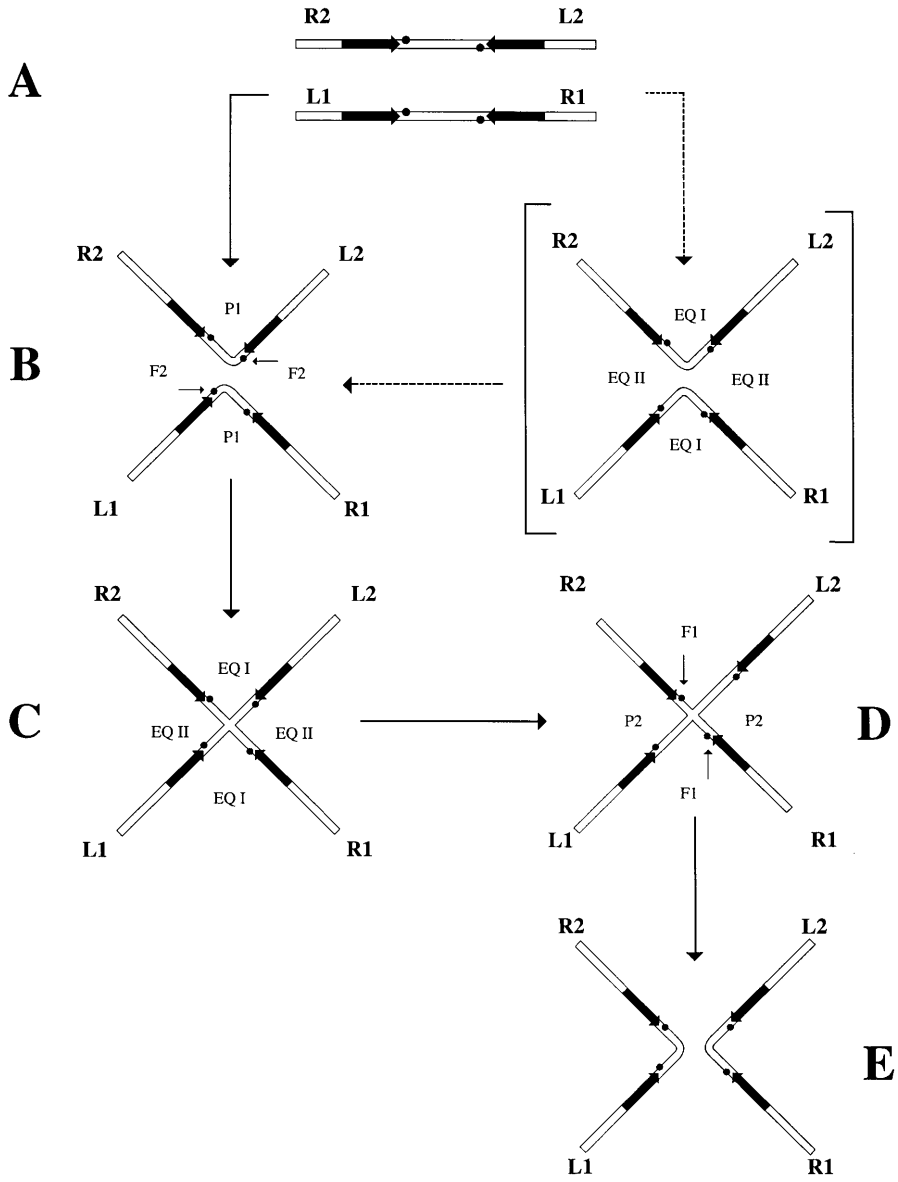

Figure 6. The oscillation model applied to the Flp recombination reaction. The parental linear substrates (L1R1 and L2R2) not bound by Flp are shown in (**A**). The Flp binding elements and their relative orientation are indicated by the dark rectangles and the arrowheads, respectively. The cleavage points at the left and right ends of the spacer are shown as dark circles. Upon binding Flp and synapsing (**B**), the L1-R1 arms and L2-R2 arms assume the cleavage-conducive P1 geometry. The two scissile phosphodiester bonds that are ready for breakage are indicated by the thin horizontal arrows. For clarity, the bound proteins are omitted from the figure. Although not necessarily true, it is convenient to imagine that the passage from (A) to (B) occurs via the symmetric state EQ I. By extrapolating the DNA configuration in (B) to that of a Holliday junction, one may imagine that the L2-R1 and L1-R2 arms are in the cleavage-suppressive F2 geometry. Cleavages by the active site tyrosine will be directed clockwise from R1 to L1 and R2 to L2, corresponding to the *trans*-horizontal mode (21). Following strand exchange, the resultant Holliday junction assumes the equilibrium state (EQ I/EQ II) by rotational branch migration (**C**). During this process, the right cleavage points approach each other and the left cleavage points move away from each other until all four are equidistant from the branch point. If, from this pseudo four-fold symmetric state, the junction oscillates back to the P1/F2 zone (analogous to the situation in B), the exchange reaction can be reversed by cleavage and joining to the parental state. If the junction migrates into the P2/F1 zone (by the right cleavage points approaching each other) (**D**), the reaction proceeds further in the forward direction. Note that the cleavage-conducive P2 state is established between the L2-R1 and L1-R2 arms. Under this condition, the L1-R1 and L2-R2 arms are in the cleavage-refractory F1 state. As a result, the direction of cleavage by the catalytic tyrosine will be from L2 to R1 and L1 to R2 (*trans*-diagonal). Subsequent strand joining completes one round of recombination and yields L1R2 and R2L1 (**E**). It should be pointed out that the recombination event, in principle, may also be accomplished by establishing the P2 state in the parental substrate and the P1 state in the Holliday intermediate, i.e. by the reverse order of strand exchange. An important outcome of the oscillation model (which assumes that the DNA arms are essentially in one plane during recombination) is that the reaction utilizes two types of dimer interactions, *trans*-horizontal and *trans*-diagonal. Note that the model will also accommodate a scheme that utilizes *trans*-diagonal cleavage between synapsed partners for the first exchange step and then *trans*-horizontal cleavage for the resolution step.

domains of the four Cre monomers are located in one plane and on the same face of the DNA (18). Since this arrangement closely resembles the EQ I/EQ II state, a simple interpretation of the structure would be that the cleavage conditions for Cre are only infinitesimally displaced from the EQ I and EQ II states. Therefore, the extent of oscillation from EQ (or the amount of branch

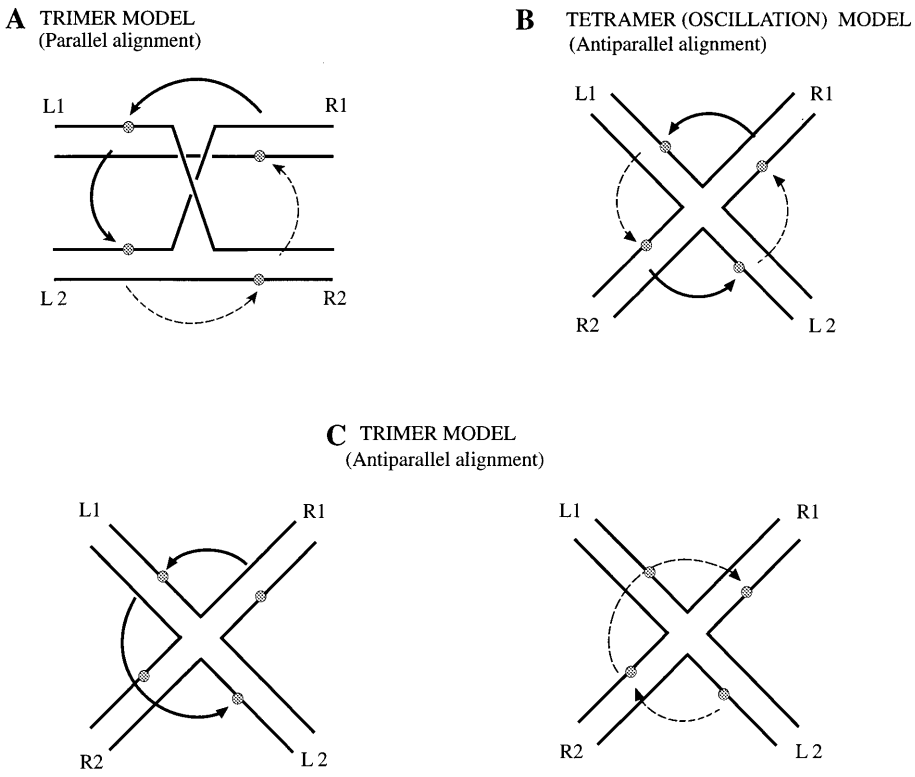

Figure 7. Functional interactions between recombinase monomers in the trimer and the tetramer (also the oscillation) models for Flp recombination. The arms of the Holliday junction are placed in the parallel orientation in (**A**) and in the antiparallel orientation in (**B**) and (**C**). The functional interaction between two Flp monomers is indicated by the direction of the arrow denoting the donation of the active site tyrosine from one to the other. The proteins bound to the DNA arms are omitted for clarity. The cleavage events at the left end of the spacer (on the L1 and L2 arms) are shown by the bold arrows; those at the right end of the spacer (on the R1 and R2 arms) are shown by the dashed arrows. The trimer model (51) operating on the parallel Holliday junction (A) or on the antiparallel Holliday junction (C) utilizes two cleavage modes (*trans*-horizontal and *trans*-vertical) for each pair of strand cleavages. The oscillation model (B) utilizes all four monomers of Flp but only one cleavage mode for each pair of strand cleavages (*trans*-horizontal at the left end of the spacer and *trans*-diagonal at the right end).

migration) during Cre recombination must be close to zero, or at least quite small. This limited branch migration, coupled with scissor-like movement of the DNA arms (18), may be sufficient to introduce the asymmetry required for discriminative left or right cleavages in this system. Thus, in their cleavage configuration, two adjacent recombinase binding planes represented by the Va^L and Va^R vectors (shown in red in Fig. 2B) must be only slightly displaced from the equilibrium positions of the corresponding planes represented by the Vc^L and Vc^R vectors (shown in green in Fig. 2B). In order to obtain this presumably uniform cleavage condition for the Int family, the vectors Va for a given member, as depicted in Figure 2B, must be rotated so that they tend towards coincidence with Vc. The following inferences can then be made regarding the extent of branch migration in individual recombination systems. Since the binding planes 1 (Va^L, Va^R) have an angular displacement of 36° and 72° for Int and Flp (compared with nearly 0° for Cre), each must rotate through an additional 18° and 36°, respectively, towards each other to assume their catalytically functional configuration. These rotations correspond to branch migrations of ~0.5 and 1 bp to the left or to the right of the equilibrium state EQ I/EQ II. Thus, in order to switch the recombination system from the cleavage state that leads to Holliday junction formation to the cleavage state that leads to its resolution, the range of branch migration (or the amplitude of oscillation) for Int and Flp must be, respectively, 1 and 2 bp greater than that for Cre. If we accept that the extent of branch migration during Cre recombination is 0–1 bp, the corresponding values for Int and Flp must be 1–2 and 2–3 bp, respectively. In the case of Int, there is direct experimental evidence that location of the crossover point immediately to the left or to the right of the central base pair of the 7 bp long spacer strongly biases resolution of the Holliday junction to the left or to the right, respectively (39). Similarly, the inferred extent of branch migration during Flp recombination is ~2–3 bp (45). One may generalize these results to state that, for members of the Int family that have the same spacer length, the extent of branch migration during recombination will be the same. The magnitudes of branch migration according to the model would be ~0–1, 1–2 and 2–3 bp for spacer lengths of 6–8 bp, respectively.

A significant aspect of the oscillation model is that the predicted range of branch migration in every recombination system is shorter than the spacer length by ~5–6 bp. Therefore, branch migration (which is confined to the central region of the spacer according to the model) alone cannot account for the complete exchange of the spacer DNA between two recombining partners. A simple solution to this problem would be to swap equal segments of 2.5–3 bp at each end of the spacer following strand cleavage, but prior to the strand joining step. The first swap would take place just before the formation of the covalently closed Holliday junction and the second swap would occur at the time of its resolution. This quantized mode of strand exchange is consistent with the results obtained for the Flp, Int and

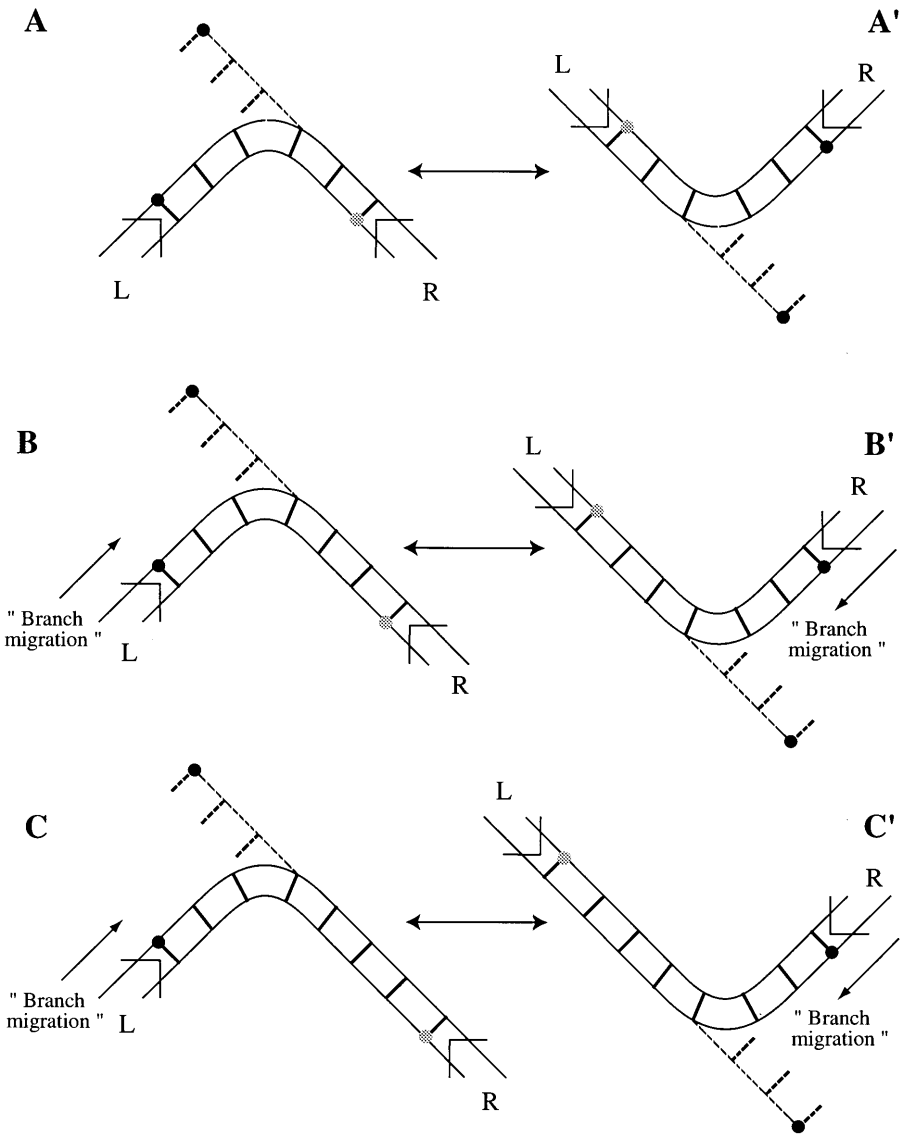

Figure 8. Establishment of DNA bend locations for strand cleavage by the Int family recombinases. For the left end cleavage, the DNA bend is located ~3 bp away from the top strand scissile phosphate for Cre (6 bp spacer) (**A**), Int (7 bp spacer) (**B**) and Flp (8 bp spacer) (**C**). The bend disposition of the DNA arms for the right end cleavage are shown in (**A′**)–(**C′**). The dark circle represents the scissile phosphodiester bond whose cleavage is imminent. The gray circle indicates the scissile phosphodiester bond that is cleavage-refractory under a given DNA configuration. The left panel represents the cleavage state in the P1 zone (see text); the right panel represents the cleavage state in the P2 zone. The P1 to P2 transition or vice versa requires either the crossing of the switch point SP-P as shown in Figure 5B or alternative modes of DNA bending analogous to that depicted in Figure 3C. For a DNA molecule with the bend located exactly at the center of the spacer (equidistant from the labile phosphates), asymmetry in the bend placement can be effected by relative rotation of the DNA arms (along with the bound recombinase monomers) in a manner analogous to branch migration within the Holliday junction intermediate. Torsional stress in the bent DNA may facilitate joining of the cleaved strands in the recombinant mode (by using a spring-like mechanism to initiate strand exchange between substrate partners and by a latch-like mechanism to resolve the Holliday intermediate).

XerC/XerD systems (39,44,45,52) and with the structure of the cleaved Cre–DNA complex (18).

DNA bending in strand swapping: 'springs and latches'

According to the model, the cleavable position of the scissile phosphate is located almost exactly 3 bp away from the bend center in the linear substrate (or 3 bp away from the branch point of the Holliday junction), which is ideal for a 6 bp spacer (Cre or XerC/XerD) (Fig. 8A). For a 7 (Int) or 8 bp (Flp) spacer, the scissile phosphate will have to move (or branch migrate) through ~0.5 or 1 bp, respectively, towards the bend center to achieve the same end (Fig. 8B and C). Figure 8 also illustrates how, in a two armed substrate, the two alternative cleavage states can be arrived at by DNA rotation across the switch point or by distinct modes of relative bending between two DNA arms. Whereas Figure 8A–C represents the conditions for left end cleavage within the P1 zone, Figure 8A′–C′ represents those for right end cleavage within the P2 zone (Fig. 6). As already pointed out, once the first exchange of strands has been completed during a normal reaction, it may be quite difficult, within the Holliday junction, to traverse the switch point without running into steric conflicts. However, the four-armed

junction is ideally configured to shifting from one cleavage state to the other by one DNA arm switching its partnership between two adjacent DNA arms (from *trans*-horizontal to *trans*-diagonal or vice versa; Fig. 6).

The release of tension harnessed in the bend upon strand cleavage can, in principle, be utilized for propelling 2.5–3 nt segments away from their original partner strands and towards their new partners at the initiation and termination steps of the reaction pathway (33). A DNA 'spring' may be established at one end of the spacer, if an intrinsic sequence-dependent bend at that position is opposed by the bend induced upon recombinase binding. The first pair of strand cleavages, followed by Holliday formation, would dissipate the accumulated torsional stress. Following the second pair of cleavages, the broken strands would reseal in a 'latch-like' manner to produce the recombinant products. We note that differences in the bend-induced tension at the two ends of a spacer (spring-like or latch-like) could impart a prescribed order of strand exchange to a recombination system.

SUMMARY

The 'oscillation model' derives its name from the potential oscillatory movements of the DNA cleavage points within the Holliday intermediate formed during recombination. It should be clarified that one recombination event requires only one swing of the reaction complex from the initiation to the termination state, or one half oscillation.

The global geometries of the cleavage-permissive and cleavage-forbidden states (P and F) proposed by the model can be related to the molecular mechanisms that restrict strand cleavage and exchange to only one end of the spacer at a time. In the Flp system, the bound Flp dimer activates the scissile phosphodiesters at both spacer ends and half-of-the-sites activity results from the misorientation of one of the two catalytic tyrosines (34). This active site selectivity is readily accommodated by the two-fold DNA–protein symmetry seen in the Cre recombination complex (18,37). However, the structures of recombination intermediates formed by several members of the Int family would be useful in generalizing the nature and positioning of the DNA bends during the reaction.

In principle, an Int family recombination model that involves little or no branch migration (*a la* Cre) is still possible, provided the geometry of recombinase–DNA association in individual systems has been precompensated for their differences in the spacer lengths. In this case, the relative orientations of Va^{L} and Va^{R} for the DNA-bound recombinase dimer would be the same for all systems. Since the length of the swapped DNA segments at the initiation and termination steps appears to be the same (3 bp) for Cre, Int and Flp, despite the differences in their spacer lengths (6, 7 and 8 bp), we tend to favor the limited branch migration model.

ACKNOWLEDGEMENTS

We thank Lorenzo Sadun, John Luecke, Dorothy Buck, Isabel Darcy and Ian Grainge for stimulating discussions and incisive criticisms. We also acknowledge all remarks received from several sources, some kind and some unkind, on a previous version of the manuscript. We have kept them in mind in our attempt to improve the clarity of presentation. We thank Laurence Hurley and the Drug Dynamics Group at UT Austin for use of their molecular graphics facility. This work was supported by a grant from the National Institutes of Health. Partial support was provided by the Robert F. Welch Foundation.

REFERENCES

1 Landy,A. (1993) *Curr. Opin. Genet. Dev.*, **3**, 699–707.
2 Sadowski,P.D. (1993) *FASEB J.*, **7**, 760–767.
3 Futcher,A.B. (1986) *J. Theor. Biol.*, **119**, 197–204.
4 Volkert,F.C. and Broach,J.R. (1986) *Cell*, **46**, 541–550.
5 Craig,N.L. (1988) *Annu. Rev. Genet.*, **22**, 77–105.
6 Sherratt,D.J. (1993) *Nucleic Acids Mol. Biol.*, **7**, 202–216.
7 Nash,H.A. (1996) *Escherichia coli and Salmonella Cellular and Molecular Biology*. ASM Press, Washington, DC, Vol. 2, pp. 2363–2376.
8 Sauer,B. (1987) *Mol. Cell. Biol.*, **7**, 2087–2096.
9 Sauer,B. and Henderson,N. (1988) *Proc. Natl Acad. Sci. USA*, **85**, 5166–5170.
10 Golic,K.G. and Lindquist,S. (1989) *Cell*, **59**, 499–509.
11 O'Gorman,S., Fox,D.T. and Wahl,G.M. (1991) *Science*, **251**, 1351–1355.
12 Kilby,N.J., Snaith,M.R. and Murray,J.A. (1993) *Trends Genet.*, **9**, 413–421.
13 Esposito,D. and Scocca,J.J. (1997) *Nucleic Acids Res.*, **25**, 3605–3614.
14 Nunes-Duby,S.E., Kwon,H.J., Tirumalai,R.S., Ellenberger,T. and Landy,A. (1998) *Nucleic Acids Res.*, **26**, 391–406.
15 Kwon,H.J., Tirumalai,R., Landy,A. and Ellenberger,T. (1997) *Science*, **276**, 126–131.
16 Hickman,A.B., Waniger,S., Scocca,J.J. and Dyda,F. (1997) *Cell*, **89**, 227–237.
17 Subramanya,H.S., Arciszewska,L.K., Baker,R.A., Bird,L.E., Sheratt,D.J. and Wigley,D.B. (1997) *EMBO J.*, **16**, 5178–5187.
18 Guo,F., Gopaul,D.N. and van Duyne,G.D. (1997) *Nature*, **389**, 40–46.
19 Argos,P., Landy,A., Abremski,K., Egan,J.B., Haggard-Ljungquist,E., Hoess,R.H., Kahn,M.L., Kalionis,B., Narayana,S.V., Pierson,L.S., Sternberg,N. and Leong,J.M. (1986) *EMBO J.*, **5**, 433–440.
20 Abremski,K. and Hoess,R.H. (1992) *Protein Engng*, **5**, 87–91.
21 Chen,J.-W., Lee,J. and Jayaram,M. (1992) *Cell*, **69**, 647–658.
22 Nunes-Duby,S.E., Tirumalai,R.S., Dorgai,L., Yagil,E., Weisberg,R.A. and Landy,A. (1994) *EMBO J.*, **13**, 4421–4430.
23 Han,Y.W., Gumport,R.I. and Gardner,J.F. (1993) *EMBO J.*, **12**, 4577–4584.
24 Arciszewska,L.K. and Sherratt,D.J. (1995) *EMBO J.*, **14**, 2112–2120.
25 Shaikh,A.C. and Sadowski,P.D. (1997) *J. Biol. Chem.*, **272**, 5695–5702.
26 Jayaram,M. (1997) *Science*, **276**, 49–51.
27 Pan,G., Luetke,K. and Sadowski,P.D. (1993) *Mol. Cell. Biol.*, **13**, 3167–3175.
28 Lee,J., Whang,I., Lee,J. and Jayaram,M. (1994) *EMBO J.*, **13**, 5346–5354.
29 Voziyanov,Y. and Kornelyuk,A.I. (1996) *Biopolymers Cell*, **12**, 17–26.
30 Umlauf,S.W. and Cox,M.M. (1988) *EMBO J.*, **7**, 1845–1852.
31 Schwartz,C.J. and Sadowski,P.D. (1989) *J. Mol. Biol.*, **205**, 647–658.
32 Schwartz,C.J. and Sadowski,P.D. (1990) *J. Mol. Biol.*, **216**, 289–298.
33 Luetke,H.L. and Sadowski,P.D. (1995) *J. Mol. Biol.*, **251**, 493–506.
34 Lee,J., Tonozuka,T. and Jayaram,M. (1997) *Genes Dev.*, **11**, 3061–3071.
35 Lee,J., Voziyanov,Y., Pathania,S. and Jayaram,M. (1998) *Mol. Cell*, **1**, 483–493.
36 White,M.F., Giraud-Panis,M.-J.E., Pohler,R.G. and Lilley,D.M.J. (1997) *J. Mol. Biol.*, **269**, 647–664.
37 Gopaul,D.N., Guo,F. and Van Duyne,G.D. (1998) *EMBO J.*, **17**, 4175–4187.
38 Stark,W.M., Sherratt,D.J. and Boocock,M.R. (1989) *Cell*, **58**, 779–790.
39 Nunes-Duby,S.E., Azaro,M. and Landy,A. (1995) *Curr. Biol.*, **5**, 139–148.
40 Chen,J.-W., Evans,B.R., Rosenfeldt,H. and Jayaram,M. (1992) *Gene*, **119**, 37–48.
41 Friesen,H. and Sadowski,P.D. (1992) *J. Mol. Biol.*, **225**, 310–326.
42 Chen,J.-W., Evans,B.R., Zheng,L. and Jayaram,M. (1991) *J. Mol. Biol.*, **218**, 107–118.
43 Azaro,M. and Landy,A. (1997) *EMBO J.*, **16**, 3744–3755.
44 Arciszewska,L.K., Grainge,I. and Sherratt,D.J. (1997) *EMBO J.*, **16**, 3731–3743.
45 Lee,J. and Jayaram,M. (1995) *J. Biol. Chem.*, **270**, 4042–4052.
46 Burgin,A.B.,Jr and Nash,H.A. (1995) *Curr. Biol.*, **5**, 1312–1321.
47 Voziyanov,Y., Lee,J., Whang,I., Lee,J. and Jayaram,M. (1996) *J. Mol. Biol.*, **256**, 720–735.
48 Lee,J., Whang,I. and Jayaram,M. (1996) *J. Mol. Biol.*, **257**, 532–549.
49 Dixon,J.E., Shaikh,A. and Sadowski,P.D. (1995) *Mol. Microbiol.*, **18**, 449–458.
50 Lee,J. and Jayaram,M. (1997) *Genes Dev.*, **11**, 2438–2447.
51 Qian,X.-H. and Cox,M.M. (1995) *Genes Dev.*, **9**, 2053–2064.
52 Zhu,X.D., Pan,G., Luetke,K. and Sadowski,P.D. (1995) *J. Biol. Chem.*, **270**, 11646–11653.